©2024 Society of Economic Geologists, Inc.
Economic Geology, v. 119, no. 6, pp. 1355–1368

Tracing the Origin of Metal Ions in Mississippi Valley-Type Ore Deposits: Constraints from Lead Isotope Studies of Black Shales from the Midcontinent United States

Noah Morris,[1,†] Adriana Potra,[1] and John R. Samuelsen,[2,3]

[1]*Department of Geosciences, University of Arkansas, Fayetteville, Arkansas 72701*

[2]*Arkansas Archeological Survey, Fayetteville, Arkansas 72704*

[3]*Department of Anthropology, University of Arkansas, Fayetteville, Arkansas 72701*

Abstract

Mississippi Valley-type (MVT) lead-zinc ore deposits found in the midcontinent United States have isotopic signatures that indicate the potential involvement of a single highly radiogenic source mobilized by hydrothermal fluids or the mixing of two sources of Pb with differing radiogenic signatures. A genetic link between black shales and major MVT ores has been thought to exist because of (1) the presence of mature hydrocarbon and brine fluid inclusions within many MVT ores, (2) the association of the hydrothermal fluids that are linked to MVT ore formation with organic compounds and oil-like droplets, and (3) the highly radiogenic nature of the ores. The analysis of 69 shale samples from 21 stratigraphic units from across the midcontinent United States revealed variations in Pb concentrations and isotopic compositions across different Cambrian- to Pennsylvanian-age shales. Shales with high organic carbon content, particularly those of Pennsylvanian age, displayed elevated Pb abundances, suggesting their formation under anoxic conditions was conducive to the preservation of organic carbon binding with Pb ions. However, the Pb isotope signatures of most black shales are generally less radiogenic than the ores, suggesting that they were not a source of radiogenic Pb. Several samples of the Devonian-Mississippian Chattanooga Shale and the Ordovician Polk Creek Shale have significant quantities of radiogenic Pb that more closely resemble those of the MVT ores. This suggests that certain shales may have directly interacted with the hydrothermal fluids that precipitated the MVT ores. Some shales may have acted as an aquitard as the hydrothermal fluids were migrating through the subsurface, causing some shales to become more enriched in radiogenic Pb than others.

Introduction

The formation of Mississippi Valley-type (MVT) lead-zinc (Pb-Zn) ores is complex, involving an interaction of tectonic compression, hydrothermal fluid migration, and geochemical processes within the subsurface. Fundamental questions regarding this interaction remain unclear, including the source(s) of the Pb and Zn ions that make up the ores.

In addition to the major ore districts hosted in carbonate sequences (Fig. 1), the midcontinent region hosts multiple trace mineralizations extending from Oklahoma to Illinois. The trace mineralizations could be MVT mineralization, sedimentary exhalative equivalents of MVT ores (Carne and Cartho, 1982), or Kupferschiefer-type shales (Coveney, 2003). Some of the Pennsylvanian shales in the region (e.g., Oklahoma, Kansas, Nebraska, Iowa, Missouri, Illinois) show high concentrations of sphalerite and are of two types: Mecca-type (Middle Pennsylvanian) and Heebner-type (Upper Pennsylvanian) (Coveney and Glascock, 1989). The Mecca-type shales—which are rich in terrestrially derived organic, U, V, and Mo contents and depleted in phosphates—possibly formed in anoxic deltaic and/or shore zone environments (Coveney and Glascock, 1989; Coveney et al., 1989). In contrast, the Heebner-type shales were formed under euxinic conditions (Coveney and Glascock, 1989; Coveney et al., 1989).

A genetic link between black shales and major MVT ores has been thought to exist because of (1) the presence of mature hydrocarbon and brine fluid inclusions within many MVT ores, (2) the association of the hydrothermal fluids that are linked to MVT ore formation with organic compounds and oil-like droplets, and (3) the highly radiogenic nature of the ores. Many midcontinent MVT deposits formed along basin margins interstratified with organic-rich black shales. These shales can form laterally extensive deposits that can accumulate a variety of metals and acquire high concentrations of U and Th, which decay into radiogenic Pb.

The goal of this comprehensive Pb isotope study is to explore the geochemistry of organic-rich black shales from the midcontinent region to constrain their possible genetic relationship with MVT ores. Although not ideal, Pb isotopes currently represent the best available tracer of metal sources in hydrothermal systems. Their utility for constraining the source of associated metals Au, Ag, Cu, and Zn and other metals is limited by the assumption that Pb was derived from the same source, transported, and deposited from the same hydrothermal fluid (Tosdal et al., 1999). This assumption is mostly true, considering the similar geochemical behavior of Pb, Cu, and Zn in hydrothermal fluids (Henley et al., 1984) and the occurrence of Pb, occasionally, in the same paragenetic stages as Zn, Cu, Ag, and Cd (Bourcier and Barnes, 1987; Wood et al., 1987). However, for Au-only or Pb-poor systems this assumption may not be valid, because Pb may have been derived from rocks along the fluid channels (Powell et al., 1991). Nonetheless, the widespread occurrence of Pb in ore minerals deposited at all temperatures, coupled with the lack

---

[†]Corresponding author: e-mail, nm009@uark.edu

Digital appendices are available in the online Supplements section.

ISSN 0361-0128; doi:10.5382/econgeo.5097; 14 p.

Submitted: January 5, 2024 / Accepted: May 9, 2024

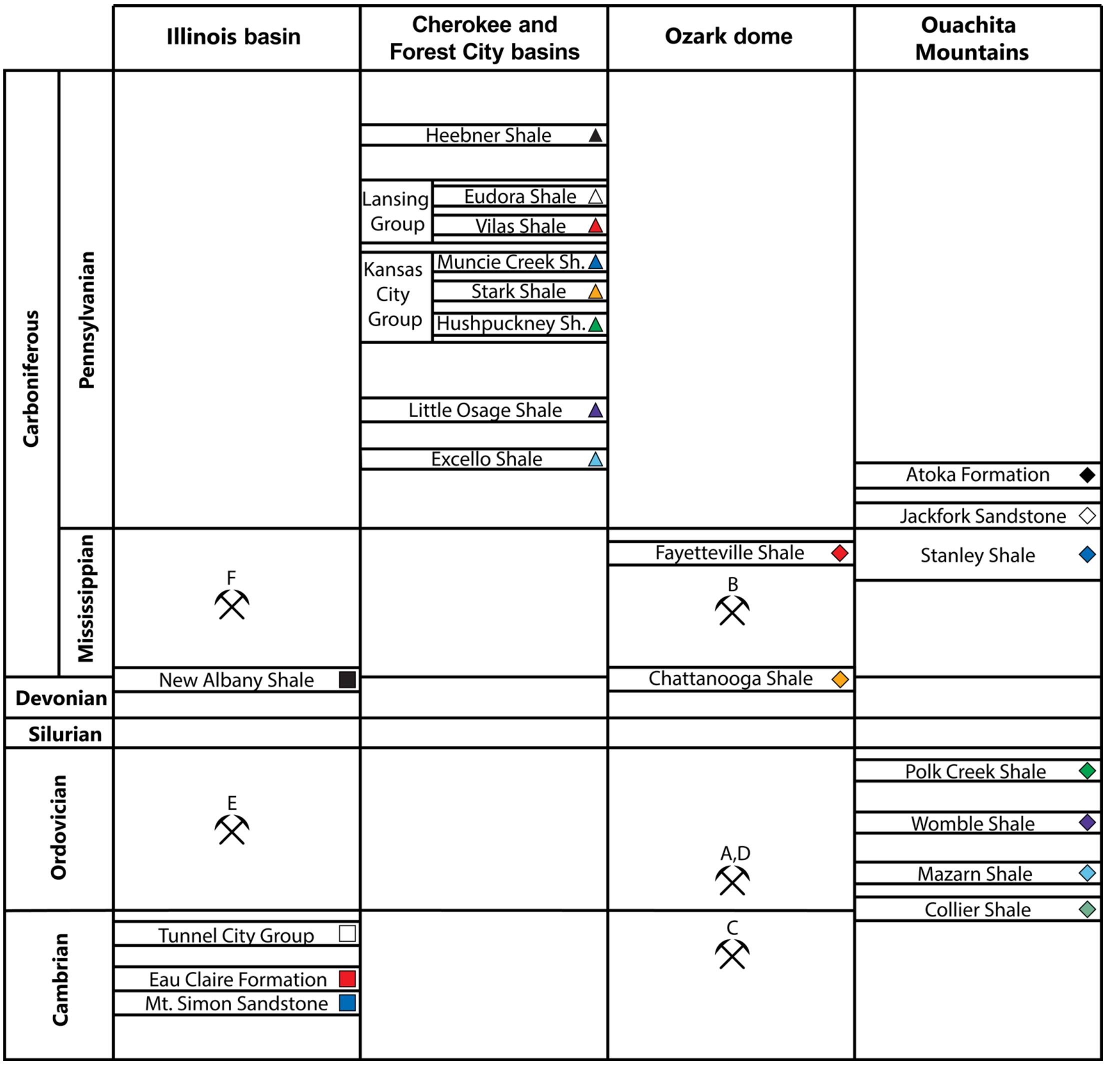

Fig. 1. Generalized stratigraphic columns of the relative ages of the sampled shales (with unique colored icons used in conjunction with Fig. 2) and the primary ore deposit host rocks in the mining districts (crossed picks): (A) Northern Arkansas, (B) Tri-State, (C) Southeast Missouri, (D) Central Missouri, (E) Upper Mississippi Valley, and (F) Illinois-Kentucky of Garven et al. (1993).

of useful isotopic variations in other metals of economic interest, makes Pb isotopes a proxy for the source(s) of associated metals (Tosdal et al., 1999). Lead isotopes are not measurably fractionated by redox reactions in solution or by fluid-mineral interactions; therefore, the isotopic composition of Pb in ores is similar to that of Pb in its source (Tosdal et al., 1999).

Of the four stable Pb isotopes, only one is nonradiogenic (^{204}Pb), whereas the other three (^{206}Pb, ^{207}Pb, and ^{208}Pb) are the product of radioactive decay of U and Th (^{238}U, ^{235}U, and ^{232}Th, respectively) (Dickin, 2005). Both U and Th typically exist in relatively high concentrations in organic-rich black shales, as they readily bind to organic matter in low-oxygen environments (Saxby, 1976; Kochenov and Baturin, 2002).

In this study, 69 samples from 21 shale and sandstone stratigraphic units from across the midcontinent United States were analyzed (Fig. 1). The samples include Cambrian- to Pennsylvanian-age samples from the Ouachita Mountains, the Ozark dome, and the Cherokee, Forest City, and Illinois basins (Fig. 2). The spatial and temporal variety of the black shales was selected for proximity to various MVT ore deposits in the midcontinent United States or description as organic-rich, metalliferous black shales (Coveney and Glascock, 1989; Coveney, 2003). Several Paleozoic shales of the Ouachita Mountain province (Collier, Mazarn, Womble, Polk Creek, Stanley, and Jackfork) have previously been analyzed for Pb isotope compositions by Simbo et al. (2019), while the Chattanooga and Fayetteville Shales of the Ozark dome province have been analyzed by Bottoms et al. (2019). This study employs many of these samples but utilizes a refined digestion method for a complete dissolution rather than partial dissolution.

Geologic Setting

The Ozark dome, located centrally in the study area, comprises uplifted Precambrian (~1.476 Ga) granite and rhyolite, along with alkaline intrusions dating to ~1.38 Ga and mafic intrusions ~1.33 Ga (Lowell and Young, 1999; Meert and Stuckey, 2002).

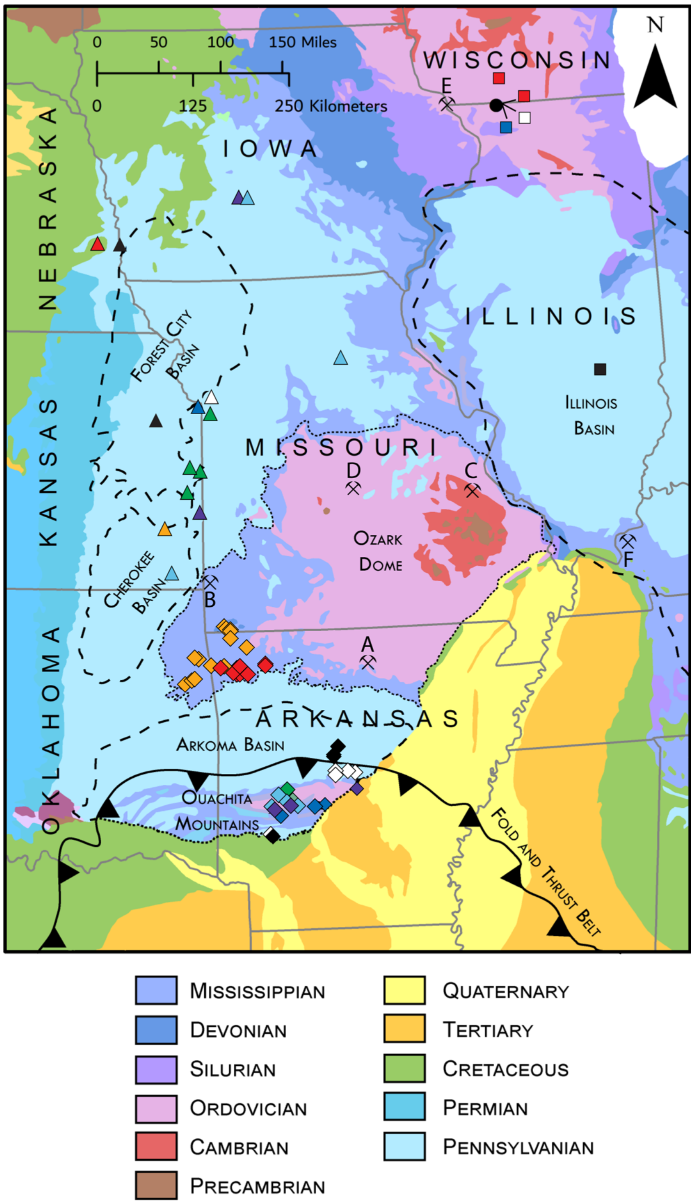

Fig. 2. Geologic map of the study area. Sampled localities marked with symbols representing stratigraphic units as in Figure 1, with major structural features indicated by dashed lines (basins), dotted lines (uplifts), and saw-toothed line (Ouachita fold-and-thrust belt). Mining districts (crossed picks) include (A) Northern Arkansas, (B) Tri-State, (C) Southeast Missouri, (D) Central Missouri, (E) Upper Mississippi Valley, and (F) Illinois-Kentucky (Garven et al., 1993).

Atop this granite and rhyolite lie sedimentary rocks from the Cambrian to Mississippian periods. The Ozark dome has an uneven structure, with Paleozoic layers sloping at less than 1° on its southwestern flank, while on the eastern side, the dome dips more steeply owing to fault zones, mainly reverse faults, and the Reelfoot rift, which separates it from the Illinois basin (Chinn and König, 1973; McBride and Nelson, 1999). These fault zones originated during the early Middle Devonian era and were preceded by the Reelfoot rift, a rift zone from late Proterozoic to early Cambrian times, now buried beneath Cretaceous and Cenozoic sediments in the northern part of the Mississippi embayment (Ervin and McGinnis, 1975; Devera and Fraunfelter, 1988; Nelson and Zhang, 1991; Parrish and Arsdale, 2004; Arsdale and Cupples, 2013). The southern portion of the Ozark dome consists mostly of E-striking normal faults alongside a mix of NE-striking strike-slip faults formed during the Ouachita orogeny (Hudson, 2000). The units sampled in this region are the Chattanooga Shale (Devonian) and the Fayetteville Shale (Mississippian).

The Ouachita Mountains are part of the Alleghanian-Ouachita-Marathon-Sonora fold-and-thrust belt, stretching from southwest Texas and northern Mexico to the southern Appalachian Mountains. These mountains resulted from the transpressional orogeny of the Laurentia and Gondwana plates during the early Carboniferous period, as the Laurentia plate subducted under Gondwana (Hatcher, 2002;

Nance et al., 2010). The collision between Laurentia and Gondwana along the southern Appalachians caused the Alleghanian orogeny (Hatcher, 2002). This collision rotated in a clockwise direction, causing the sea to close and continuing the orogeny along the fold and thrust belt. Consequently, foreland basins, such as the Arkoma basin, developed along the northern periphery of the belt. The Ouachita stratigraphy mainly comprises deep-water, turbiditic facies dominated by sandstones and shales (Morris, 1971; Owen and Carozzi, 1986; McFarland, 2004). The sampled units in the Ouachita Mountains encompass various formations from Cambrian to Pennsylvanian periods, including the Collier Shale (Upper Cambrian to Lower Ordovician), the Mazarn Shale (Lower Ordovician), the Womble Shale (Middle to Upper Ordovician), the Polk Creek Shale (Upper Ordovician), the Stanley Shale (Meramecian to Chesterian Series, Mississippian), the Jackfork Sandstone (Morrowan Series, Pennsylvanian), and the Atoka Formation (Atokan Series, Pennsylvanian).

The Illinois basin evolved because of tectonic events spanning Precambrian to Cambrian times, and subsequently with the Reelfoot rift and the Rough Creek graben formation after the breakup of a supercontinent (Klein and Hsui, 1987; Kolata and Nelson, 1990a, b). Throughout the Carboniferous and Permian periods, compressional stresses from the Alleghenian and Ouachita orogenies led to further subsidence of the Illinois basin (Klein and Hsui, 1987; Kolata and Nelson, 1990a, b). The Mt. Simon Sandstone typically overlies the Precambrian igneous basement rocks in most parts of the basin (Sargent, 1990). The Illinois basin region comprises several clastic and carbonate successions, including the Mt. Simon Sandstone (Cambrian), the Eau Claire Formation (Cambrian), the Tunnel City Group (Cambrian), and the New Albany Shale (Devonian).

The Cherokee and Forest City basins, located across Kansas, Missouri, Nebraska, and Iowa, are cratonic basins separated by the Bourbon arch, which experienced subsidence since the Cambrian, particularly accelerated during the Pennsylvanian owing to stresses from the Alleghenian and Ouachita orogenies (Jopling and Cashion, 1959; Anderson and Wells, 1968; Harris, 1985; Leighton and Kolata, 1990; Newell, 1995). The sampled stratigraphic units in the Cherokee and Forest City basins are all Pennsylvanian in age. These shales are generally referred to as a member within the state in which they were sampled, although the lithostratigraphic ranks vary across the states in which they are exposed. These units include the Excello Shale, the Little Osage Shale Member of the Marmaton Group (Desmoinesian series), the Hushpuckney, Stark, and Muncie Creek Shale Members of the Kansas City Group (Missourian series), the Vilas and Eudora Shale of the Lansing Group (Missourian series), and the Heebner Shale Member of the Shawnee Group (Virgilian series).

Mississippi Valley-Type Ore Deposits

Mississippi Valley-type ore deposits consist primarily of the lead and zinc sulfide minerals galena (PbS) and sphalerite (ZnS) that formed in epigenetic, stratabound deposits commonly hosted within carbonate rock (Leach et al., 2010a). These deposits are named after the Upper Mississippi River Valley in the United States, where numerous occurrences are found (Leach et al., 2010a). MVT deposits are generally located in large districts along basin margins or near foreland thrust belts, without any association to igneous activity and, in many instances, they are situated along basin margins where organic-rich shales overlie carbonate rocks (Leach et al., 2010a; Schutter, 2015). MVT deposits are also typically linked to solution collapse breccias, faults, or other permeable features that facilitate fluid migration (Leach et al., 2010a).

The midcontinent region, in particular the Mississippi River drainage, hosts some of the largest and best-known ore districts (Fig. 1), such as the Northern Arkansas, Tri-State, Southeast Missouri, Central Missouri, Illinois-Kentucky, and Upper Mississippi Valley districts (Leach et al., 2010a). These districts have been dated to the Pennsylvanian and early Permian, coinciding with the Ouachita orogeny (York et al., 1981; Lange et al., 1983; Wisniowiecki et al., 1983; Stein and Kish, 1985; Arbenz, 1989; Arne et al., 1990; Symons and Sangster, 1991; Arne, 1992; Hay et al., 1995; Brannon et al., 1996; Symons et al., 1998; Leach et al., 2001, 2010a; Pan et al., 2011). The Ouachita orogeny is thought to have provided the necessary tectonic controls for the migration of subsurface fluids and subsequent ore mineralization (Bradley and Leach, 2003). The orogeny was initiated by subduction and closure of an oceanic basin between Gondwana and Laurasia, followed by subsequent convergence of magmatic arcs and passive margins (Houseknecht and Matthews, 1985). During the collision of Gondwana and Laurasia, the Arkoma basin developed as a foreland basin on the northern margins of the orogenic belt, subsiding and infilling with Pennsylvanian sediments due to extensional faulting (Sutherland, 1988). The orogeny added topographic relief and increased overburden pressure on subsurface fluids, which were expelled updip to the north with the eventual precipitation of the MVT ores at lower pressures and temperatures (Fig. 3) (Garven et al., 1993; Leach et al., 2010b). The migrating warm fluids would partially dissolve the carbonate host rock, potentially further creating solution collapse breccias, allowing space for the precipitation of ore deposits (Leach et al., 1975; Plumlee et al., 1994). Locally, within individual districts and deposits, but not necessarily on a regional (basinal) scale, the hydrothermal fluid flow was primarily confined to fractures, faults, and brecciated zones, which allowed permeability for fluid flow (Appold and Garven, 1999; Appold and Nunn, 2005). Fluid inclusions in the MVT ores indicate that the temperatures of the hydrothermal fluids ranged from approximately 50° to 250°C—temperatures that are higher than the expected geothermal gradients and the burial temperatures of the host rock during ore mineralization (Basuki and Spooner, 2004; Leach et al., 2010a). This suggests that fluids may have originated from deeper basinal sources or from the basement (Leach et al., 2010a). Fluid migration through aquifers may have been constrained by shales and facilitated by faults and fractures (Appold and Nunn, 2005). Lead is soluble and mobile in aqueous solution under moderate to high temperatures (200°–600°C), whereas at low temperatures it tends to be insoluble as it readily bonds with organic matter (Tosdal et al., 1999). Fluid inclusions also indicate 10 to 30 wt % NaCl equiv salinity, which is found to be sufficient for transporting Pb and Zn as chloride complexes with fluids at MVT ore-forming temperatures (Yardley, 2005; Leach et al., 2010a). Dolomitization associated with hydrothermal fluids and MVT mineralization is known in the Knox

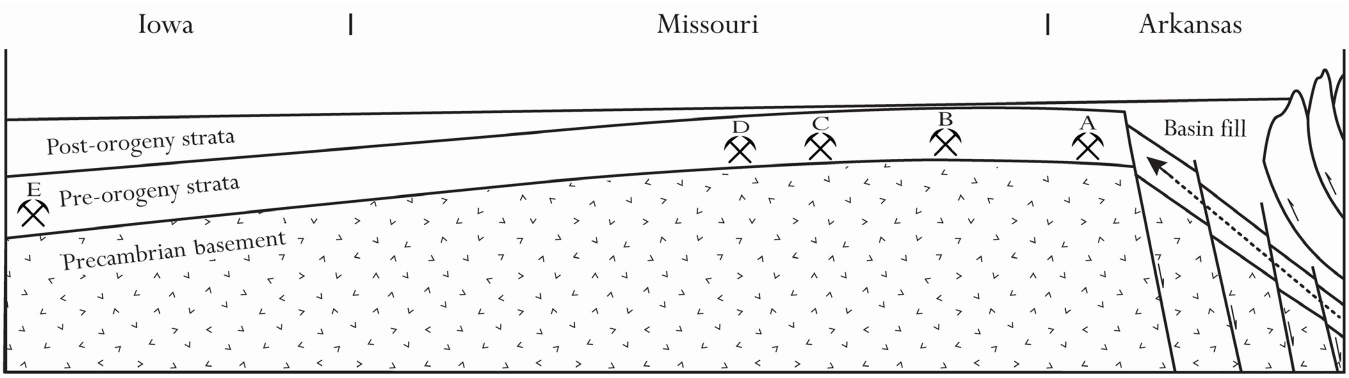

Fig. 3. Generalized cross section of the study area illustrating the subsurface fluid flow expulsion to the north during the Ouachita orogeny toward the (A) Northern Arkansas, (B) Tri-State, (C) Southeast Missouri, (D) Central Missouri, and (E) Upper Mississippi Valley mining districts.

Group of the southern Appalachians, possibly resulting from multiple pulses of hydrothermal fluids interacting with host carbonates, and may have also occurred in the Ozark carbonates (Montanez, 1994; Chick et al., 2021).

Methodology

This study utilized 69 shale samples originating from 21 shale formations located throughout the midcontinent region of the United States (Fig. 1). Samples were predominantly obtained from outcrops in Arkansas, Iowa, Kansas, Missouri, Nebraska, and Oklahoma (Fig. 2; App. Table A1). All samples came from exposures where fresh samples were able to be collected by removing as much of the exposed surface as possible using conventional hand tools to extract the least weathered samples from behind the outcrop exposure. When available, type sections or type localities were chosen for sampling. The type locality of the following shales were sampled during August 2020: Stark (near Stark, Neosho County, Kansas) (Moore, 1932; Jewett, 1933), Hushpuckney (railway cut, center north side, section 13, T19S, R23E, Miami County, Kansas) (Moore, 1932), Muncie Creek (Muncie Creek, east of Muncie, Kansas, in southern part of Wyandotte County, Kansas) (Moore, 1932), and Fayetteville (near Fayetteville, Washington County, Arkansas) (Simonds, 1891). The Excello Shale was sampled around 1.5 miles from the type section described in Searight (1955) (NW/4 section 30, T56N, R14W, 2.6 miles west of U.S. Highway 63, west of Excello, Macon County, Missouri, in highwall of coal strip pit).

Four additional samples originated from the Commonwealth Edison UPH-1 core in northern Illinois (Wisconsin Geological and Natural History Survey [WGNHS] identification number [ID] 33000331) and one additional sample from the WGNHS Highway A Quarry 2 core from southern Wisconsin (WGNHS ID 25000529). The core samples were donated by the Wisconsin Geological and Natural History Survey to provide additional geochemical data for shales in the northern Mississippi River Valley. Samples from these cores include the Eau Claire, Tunnel City, and Mt. Simon units and have been part of a previous Pb isotope study (Doe et al., 1983). One other sample, representing the New Albany Shale, originated from well cuttings from the Morris no. 1 well drilled by Ceja Corporation in 2012 in Shelby County, Illinois (American Petroleum Institute no. 12-173-24362). One of the authors was present at the time of drilling and collected this sample after cleaning it from water-based drilling mud. In sum, seven shales have only one sample from each (Mt. Simon and Tunnel City [Cambrian], Collier [Cambrian-Ordovician], New Albany [Devonian], and Muncie Creek, Stark, and Vilas [Pennsylvanian]), so they cannot be used to draw inferences, but they can be used to compare with the other temporally and spatially related shale units in this study.

Samples were rinsed with deionized water, dried, and then powdered in an alumina-ceramic dish using a Spex Sample-Prep Shatterbox. All further processing of the samples was conducted in a class 100 clean room at the University of Arkansas to reduce potential environmental contamination, and all labware used for chemical processing of the samples was acid cleaned to minimize possible contamination. All acids used in the chemical processing were previously distilled in dedicated HNO_3 and HCl Savillex DST-1000 acid purification systems.

An amount of 100 mg of power from each sample was placed in a PFA liner of a Parr acid digestion vessel (model 4749). A volume of 2 mL of reverse aqua regia was added to each sample, followed by 2 mL of concentrated HF. Each sample was left uncovered for 10 min to vent volatile gases. The samples in the liners were inserted into the acid digestion vessels and tightened. The vessels were placed in a Lindberg Blue M 828 oven and heated to 200°C for 8 h. After the vessels were allowed to cool for 24 h, the liners were extracted and placed in a fume hood in the clean room. The solution in each liner was pipetted into a 30-mL PFA vial and dried at 90°C. Each sample had 4 mL of distilled HNO_3 added, was heated to 150°C for 8 h while tightly capped, and was subsequently dried at 90°C. Four milliliters of distilled HCl was then added and heated to 150°C for 8 h while capped, then dried at 90°C. This process of adding HNO_3 and HCl was repeated once more. After each addition of heat, the samples cooled to room temperature, and after each addition of acid, the samples were allowed to remain uncovered for 10 min to remove any volatile gases.

Elemental concentration data was acquired by redissolving the dried, digested samples in 2 mL 2% HNO_3 at 150°C for 1 h. Then, a volume of 0.1 mL of each sample solution was transferred to clean 5-mL centrifuge tubes and diluted with 2.9 mL 2% HNO_3. The samples were analyzed on a Thermo-

Scientific iCAP Q inductively coupled plasma-mass spectrometry (ICP-MS) instrument at the University of Arkansas Trace Element and Radiogenic Isotope Lab. In addition, two sets of ICP-MS multielement solution standards were made using 10 ppm of Inorganic Ventures IV-ICPMS-71B and 10 ppm of HPS High Purity Standards ICP-MS-68A-A-100 diluted to multiple concentrations (500, 100, 50, 10, 5, and 1 ppb and 10 ppt). Seven duplicate samples and five replicate samples were also analyzed; these samples were chosen based on age, number of samples for each shale, and total mass of each sample available.

Following the chemical processing stage, 2 mL of double-distilled HNO_3 were added to each sample for redissolution and heated at 175°C for 2 h. Extraction of isotopes followed the protocol outlined in Pin et al. (2014). Upon extraction of Pb, the samples were dried down at 80°C. Prior to multicollector (MC)-ICP-MS analysis, they were capped and redissolved in 2 mL of 2% HNO_3 at room temperature. Immediately prior to the Pb isotope analysis, the Pb fractions were diluted to varying concentrations according to the whole-rock Pb concentrations in the digested samples analyzed on a ThermoScientific iCAP Q ICP-MS at the Trace Element and Radiogenic Isotope Laboratory at the University of Arkansas. Each diluted Pb isotope fraction was then spiked with Tl (thallium) to correct for internal mass fractionation and analyzed on a NuPlasma MC-ICP-MS instrument, also at the Trace Element and Radiogenic Isotope Laboratory. For each sample, 60 Pb ratio data points were measured and averaged; the same was also done for each of the standards (App. Table A2). Raw isotopic data were corrected using sample-standard bracketing along with the Pb standard values from Todt et al. (1996).

Total organic carbon was evaluated using dry, powdered samples placed within a tin capsule and weighed on a Sartorius ISO 9001 microbalance. The samples were analyzed on a ThermoScientific EA IsoLink IRMS CN system (includes Flash isotope ratio mass spectrometry [IRMS] elemental analyzer, Delta V IRMS, and Conflo IV Universal Interface) at the University of Arkansas Stable Isotope Laboratory. The samples were calibrated with 27 internal Silty Soil standard samples (avg 2.19 wt %; $\sigma = 0.071$).

Results

The early Paleozoic shales tend to have relatively low Pb concentrations, with the Cambrian shales having 3 to 14 ppm and the Ordovician shales ranging from 0.9 to 16 ppm (Table 1). The Devonian shale samples vary between 8 and 29 ppm of Pb, with one sample of the basal Chattanooga Shale (CS10B) yielding 62 ppm Pb. The Mississippian shale samples range in Pb concentrations from 6 to 22 ppm. The Pennsylvanian shale samples with high organic content have the highest Pb abundances. As such, the Pennsylvanian shales of the Ouachita Mountains (Jackfork and Atoka) have 10 to 16 ppm Pb, whereas the Pennsylvanian shales of the Cherokee and Forest City basins display a wide range of Pb content ranging from 13 to 240 ppm.

The Th concentrations of all samples range from less than 1 to 20 ppm and are relatively consistent among all samples (Table 1). The U concentrations range from less than 1 ppm to 49 ppm, with the total organic carbon-rich Pennsylvanian shales (>5 wt %) exhibiting the most elevated concentrations. Similarly, the Zn concentrations vary between the following values: the Cambrian-Ordovician samples between 3 and 93 ppm Zn, the Devonian samples between 45 and 245 ppm Zn, the Mississippian samples between 52 and 741 ppm Zn, and the Pennsylvanian samples between 57 and 3,051 ppm.

The Pb isotope ratios of whole-rock shales were determined and subsequently age-corrected to the estimated time of ore genesis, approximately 250 m.y. (Table 1) (Pan et al., 1990; Brannon et al., 1996). Within the Cambrian Mt. Simon, Eau Claire, and Tunnel City samples, the $^{208}Pb/^{204}Pb$ ratios vary between 37.713 and 41.272, encompassing the uppermost values observed in the analyzed shales. Their $^{207}Pb/^{204}Pb$ and $^{206}Pb/^{204}Pb$ ratios range from 15.299 to 15.880 and 17.566 to 21.465, respectively. The Ordovician shales exhibit $^{208}Pb/^{204}Pb$ ratios spanning from 37.856 to 38.080, $^{207}Pb/^{204}Pb$ ratios from 15.508 to 15.971, and $^{206}Pb/^{204}Pb$ ratios from 17.890 to 19.952. Among the Ordovician shales, the Polk Creek Shale records the highest $^{207}Pb/^{204}Pb$ and $^{206}Pb/^{204}Pb$ values. The Devonian Chattanooga and New Albany shales yield $^{208}Pb/^{204}Pb$ ratios varying from 38.042 to 40.596, $^{207}Pb/^{204}Pb$ ratios from 15.580 to 15.863, and $^{206}Pb/^{204}Pb$ ratios from 17.104 to 21.209. The Mississippian Fayetteville and Stanley shales exhibit Pb isotope ratios that closely resemble each other, with the Stanley Shale showing marginally higher values. Specifically, the Pb isotope ratios of the Fayetteville shales range from 36.416 to 38.434 ($^{208}Pb/^{204}Pb$), 15.521 to 15.649 ($^{207}Pb/^{204}Pb$), and 16.289 to 18.745 ($^{206}Pb/^{204}Pb$), and those of the Stanley shales range from 38.471 to 38.760 ($^{208}Pb/^{204}Pb$), 15.651 to 15.674 ($^{207}Pb/^{204}Pb$), and 18.526 to 18.831 ($^{206}Pb/^{204}Pb$). The Ouachita Mountains Pennsylvanian Atoka and Jackfork shales exhibit highly comparable ratios, ranging from 38.541 to 38.883 for $^{208}Pb/^{204}Pb$, 15.629 to 15.666 for $^{207}Pb/^{204}Pb$, and 18.598 to 18.799 for $^{206}Pb/^{204}Pb$. The Cherokee and Forest City basins Pennsylvanian shales have values spanning from 37.265 to 38.643 for $^{208}Pb/^{204}Pb$, 15.560 to 15.652 for $^{207}Pb/^{204}Pb$, and 17.523 to 18.721 for $^{206}Pb/^{204}Pb$.

Discussion

The highly radiogenic characteristics of ores from the midcontinent districts are illustrated on covariate Pb isotope diagrams: $^{206}Pb/^{204}Pb$ vs. $^{207}Pb/^{204}Pb$ (uranogenic) and $^{206}Pb/^{204}Pb$ vs. $^{208}Pb/^{204}Pb$ (thorogenic). On such diagrams, the ore samples plot beyond the 0 Ma value of the theoretical upper crust and orogenic growth curves of Zartman and Doe (1981) (Fig. 4), indicating they formed at future ages and defying the average crustal signatures of radiogenic Pb. Consequently, these ores have been termed “J-type” or “Joplin-type” ores, after the Tri-State mining district city of Joplin, Missouri, to define ores that are highly enriched in ^{206}Pb, ^{207}Pb, and ^{208}Pb (Neir, 1938; Houtermans, 1953; Cannon and Pierce, 1969; Leach and Sangster, 1993). These distinctive Pb isotope signatures are indicative of a Pb source(s) enriched in ^{238}U, ^{235}U, and ^{232}Th relative to the upper crust and orogenic growth curves (Fig. 4). J-type characteristics have also been found in trace metals in localities outside of the midcontinent ore districts, suggesting widespread enrichment of radiogenic Pb in the midcontinent United States beyond basin- and ore district-scale regions (Field et al., 2020).

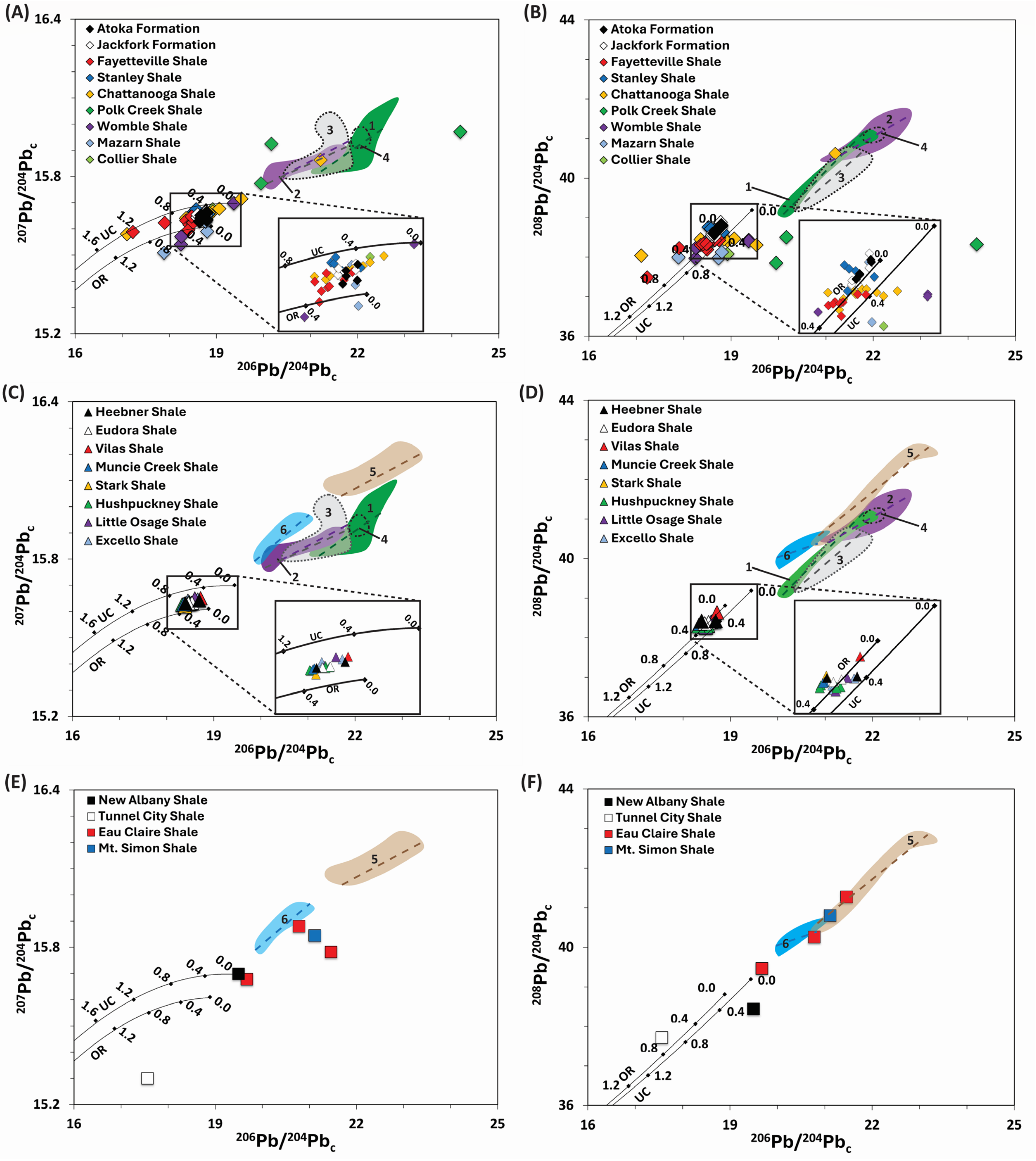

Fig. 4. Thorogenic and uranogenic diagrams depicting the Pb isotope ratios of the analyzed shale samples from the Ouachita Mountain and Ozark dome provinces (4A, B), the Cherokee and Forest City basins (4C, D), and the Illinois basin (4E, F). Also included are fields delineating the Pb isotope ratios of ore samples from major Mississippi Valley-type districts within the midcontinent United States: Northern Arkansas (1), Tri-State (2), Southeast Missouri (3), Central Missouri (4), Upper Mississippi Valley (5), and Illinois-Kentucky (6) (Heyl et al., 1966; Goldhaber et al., 1995; Bottoms et al., 2019). The theoretical growth curves over time (in Ga) of the upper crust (UC) and the orogenic mixed upper and lower crust (OR) are also represented (Doe and Zartman, 1979). Subscript c indicates corrected isotopic ratios to 250 Ma.

Table 1. Measured (present–day) and Age-Corrected (250 Ma) Pb Isotope Values

Formation/ member	Sample ID	Approximate age (Ma)	Zn (ppm)	Pb (ppm)	Th (ppm)	U (ppm)	TOC (wt %)	^{208}Pb/^{204}Pb measured	^{207}Pb/^{204}Pb measured	^{206}Pb/^{204}Pb measured	^{208}Pb/^{204}Pb age-corrected	^{207}Pb/^{204}Pb age-corrected	^{206}Pb/^{204}Pb age-corrected
Heebner	9 Heebner	300	755.1	105.5	8.7	15.9	14.78	$38.489 \pm 7.62 \times 10^{-4}$	$15.661 \pm 2.56 \times 10^{-4}$	$19.071 \pm 2.80 \times 10^{-4}$	38.421	15.641	18.690
Heebner	13 Heebner	300	2,861.6	65.8	8.3	40.8	17.68	38.511 ± 1.68 × 10–3	$15.712 \pm 6.81 \times 10^{-4}$	$19.992 \pm 9.86 \times 10^{-4}$	38.405	15.631	18.397
Heebner	13 Heebner (R)	300	3,051.4	69.5	9.5	46.0	n.d.	n.d.	n.d.	n.d.	n.d.	n.d.	n.d.
Eudora	15 Eudora	305	631.5	201.0	10.7	33.9	10.02	$38.434 \pm 7.55 \times 10^{-4}$	$15.655 \pm 2.97 \times 10^{-4}$	$18.965 \pm 3.38 \times 10^{-4}$	38.390	15.633	18.538
Eudora	21 Eudora	305	1,274.1	221.8	9.9	26.4	18.90	$38.397 \pm 5.06 \times 10^{-4}$	$15.647 \pm 1.66 \times 10^{-4}$	$18.760 \pm 2.25 \times 10^{-4}$	38.360	15.631	18.460
Vilas	15 Vilas	305	26.6	12.6	6.8	6.8	5.07	$39.094 \pm 6.98 \times 10^{-4}$	$15.722 \pm 2.73 \times 10^{-4}$	$20.110 \pm 3.59 \times 10^{-4}$	38.639	15.651	18.719
Muncie Creek	11-1 Muncie Creek	305	924.2	234.7	9.4	48.7	28.06	$38.394 \pm 9.49 \times 10^{-4}$	$15.657 \pm 3.23 \times 10^{-4}$	$18.898 \pm 4.79 \times 10^{-4}$	38.361	15.630	18.374
Muncie Creek	11-2 Muncie Creek	305	463.6	128.7	7.9	28.1	23.07	$38.401 \pm 7.76 \times 10^{-4}$	$15.656 \pm 2.79 \times 10^{-4}$	$18.911 \pm 3.66 \times 10^{-4}$	38.351	15.628	18.360
Stark	2 Stark	305	437.5	23.4	4.6	29.4	12.95	$38.596 \pm 1.03 \times 10^{-3}$	$15.789 \pm 4.17 \times 10^{-4}$	$21.693 \pm 5.61 \times 10^{-4}$	38.429	15.620	18.391
Hushpuckney	5 Hushpuckney	305	375.3	31.3	11.6	8.5	3.80	$38.615 \pm 1.09 \times 10^{-3}$	$15.670 \pm 4.08 \times 10^{-4}$	$19.184 \pm 5.09 \times 10^{-4}$	38.307	15.634	18.490
Hushpuckney	6 Hushpuckney	305	828.3	88.8	8.9	39.6	15.49	$38.408 \pm 8.38 \times 10^{-4}$	$15.684 \pm 3.35 \times 10^{-4}$	$19.472 \pm 3.99 \times 10^{-4}$	38.326	15.626	18.337
Hushpuckney	8 Hushpuckney	305	2,037.8	157.5	5.2	32.6	37.01	$38.333 \pm 8.07 \times 10^{-4}$	$15.659 \pm 3.10 \times 10^{-4}$	$19.052 \pm 3.49 \times 10^{-4}$	38.306	15.632	18.528
Hushpuckney	8 Hushpuckney (D)	305	2,190.8	165.3	5.2	40.7	n.d.	$38.331 \pm 1.05 \times 10^{-3}$	$15.663 \pm 4.17 \times 10^{-4}$	$19.115 \pm 4.88 \times 10^{-4}$	38.292	15.631	18.491
Hushpuckney	20 Hushpuckney	305	1,005.2	90.7	9.8	24.6	21.75	$38.383 \pm 7.18 \times 10^{-4}$	$15.662 \pm 2.67 \times 10^{-4}$	$19.015 \pm 2.93 \times 10^{-4}$	38.295	15.627	18.328
Little Osage	3 Little Osage	310	365.7	239.5	8.6	19.2	32.41	$38.371 \pm 1.41 \times 10^{-3}$	$15.645 \pm 5.53 \times 10^{-4}$	$18.683 \pm 6.78 \times 10^{-4}$	38.258	15.635	18.481
Little Osage	16A Little Osage	310	391.7	69.9	9.9	36.0	6.98	$38.525 \pm 8.67 \times 10^{-4}$	$15.718 \pm 3.42 \times 10^{-4}$	$19.919 \pm 4.31 \times 10^{-4}$	38.406	15.650	18.596
Excello	1 Excello	310	467.1	65.8	8.6	12.3	10.74	$38.502 \pm 1.30 \times 10^{-3}$	$15.670 \pm 4.67 \times 10^{-4}$	$19.135 \pm 5.93 \times 10^{-4}$	38.401	15.646	18.661
Excello	17 Excello	310	1,037.6	165.1	9.2	38.9	14.06	$38.369 \pm 8.83 \times 10^{-4}$	$15.672 \pm 3.45 \times 10^{-4}$	$19.047 \pm 3.78 \times 10^{-4}$	38.323	15.641	18.451
Excello	19 Excello	310	1,111.2	66.3	8.4	21.0	21.73	$38.476 \pm 8.44 \times 10^{-4}$	$15.674 \pm 3.34 \times 10^{-4}$	$19.256 \pm 3.83 \times 10^{-4}$	38.279	15.633	18.454
Atoka	UA1Sh	315	87.0	13.3	4.3	1.3	1.79	$39.062 \pm 9.13 \times 10^{-4}$	$15.675 \pm 3.31 \times 10^{-4}$	$19.052 \pm 3.43 \times 10^{-4}$	38.791	15.662	18.799
Atoka	LA1Sh	315	81.6	14.5	3.6	1.2	0.92	$39.009 \pm 8.43 \times 10^{-4}$	$15.646 \pm 3.17 \times 10^{-4}$	$19.010 \pm 3.36 \times 10^{-4}$	38.816	15.635	18.794
Atoka	LA2Sh	315	82.4	13.8	5.8	1.4	0.93	$38.999 \pm 9.35 \times 10^{-4}$	$15.655 \pm 3.17 \times 10^{-4}$	$18.935 \pm 3.68 \times 10^{-4}$	38.650	15.642	18.682
Atoka	LA2Sh (D)	315	84.7	14.1	6.3	1.5	n.d.	$39.030 \pm 1.05 \times 10^{-3}$	$15.665 \pm 4.02 \times 10^{-4}$	$18.944 \pm 4.69 \times 10^{-4}$	38.660	15.651	18.680
Atoka	Atoka 2	315	114.1	15.7	5.2	1.2	0.91	$38.876 \pm 8.46 \times 10^{-4}$	$15.638 \pm 3.07 \times 10^{-4}$	$18.839 \pm 3.58 \times 10^{-4}$	38.601	15.628	18.646
Jackfork	UJ1Sh	315	61.1	11.2	8.5	1.8	0.99	$39.222 \pm 1.30 \times 10^{-3}$	$15.676 \pm 4.32 \times 10^{-4}$	$19.024 \pm 3.72 \times 10^{-4}$	38.586	15.655	18.604
Jackfork	UJ2Sh	315	65.4	10.1	6.1	1.9	2.65	$39.231 \pm 1.67 \times 10^{-3}$	$15.688 \pm 5.71 \times 10^{-4}$	$19.248 \pm 5.30 \times 10^{-4}$	38.726	15.664	18.778
Jackfork	MJ1	315	79.3	10.9	9.1	1.8	0.80	$39.236 \pm 2.19 \times 10^{-3}$	$15.671 \pm 6.81 \times 10^{-4}$	$19.084 \pm 6.41 \times 10^{-4}$	38.543	15.649	18.662
Jackfork	MJ2	315	75.8	13.6	7.4	1.5	0.80	$38.989 \pm 1.11 \times 10^{-3}$	$15.658 \pm 3.94 \times 10^{-4}$	$18.879 \pm 4.29 \times 10^{-4}$	38.540	15.644	18.598
Jackfork	LJ1	315	57.3	10.7	3.3	0.9	0.99	$39.139 \pm 1.20 \times 10^{-3}$	$15.664 \pm 3.85 \times 10^{-4}$	$18.997 \pm 4.74 \times 10^{-4}$	38.885	15.653	18.779
Fayetteville	FS1L	325	349.0	10.9	11.7	7.8	7.38	$39.224 \pm 9.00 \times 10^{-4}$	$15.728 \pm 2.51 \times 10^{-4}$	$20.239 \pm 3.64 \times 10^{-4}$	38.310	15.632	18.361
Fayetteville	FS2U	325	116.2	21.2	13.1	2.6	1.48	$38.859 \pm 6.28 \times 10^{-4}$	$15.631 \pm 2.37 \times 10^{-4}$	$18.734 \pm 2.56 \times 10^{-4}$	38.347	15.616	18.429
Fayetteville	FS3	325	255.4	8.4	11.0	4.4	5.33	$39.288 \pm 5.98 \times 10^{-4}$	$15.691 \pm 2.29 \times 10^{-4}$	$19.833 \pm 2.81 \times 10^{-4}$	38.191	15.622	18.494
Fayetteville	FS4	325	137.6	13.6	11.0	2.5	1.77	$38.998 \pm 7.66 \times 10^{-4}$	$15.620 \pm 2.99 \times 10^{-4}$	$18.876 \pm 3.02 \times 10^{-4}$	38.327	15.597	18.409
Fayetteville	FS6L	325	280.1	6.7	9.7	9.8	8.44	$39.485 \pm 6.84 \times 10^{-4}$	$15.823 \pm 2.18 \times 10^{-4}$	$21.811 \pm 3.06 \times 10^{-4}$	38.229	15.623	17.902
Fayetteville	FS7L	325	133.4	5.6	13.3	7.2	7.03	$39.502 \pm 1.00 \times 10^{-3}$	$15.760 \pm 3.70 \times 10^{-4}$	$20.589 \pm 4.64 \times 10^{-4}$	37.485	15.588	17.229
Fayetteville	FS8UU	325	740.6	7.4	5.4	1.4	0.45	$39.032 \pm 1.18 \times 10^{-3}$	$15.674 \pm 4.58 \times 10^{-4}$	$19.239 \pm 5.45 \times 10^{-4}$	38.427	15.649	18.744
Fayetteville	FS9LU	325	127.7	13.0	8.1	1.7	1.10	$38.947 \pm 7.81 \times 10^{-4}$	$15.652 \pm 2.90 \times 10^{-4}$	$18.983 \pm 2.71 \times 10^{-4}$	38.433	15.635	18.660
Fayetteville	FS10L	325	114.3	21.7	17.0	2.6	0.70	$38.994 \pm 7.75 \times 10^{-4}$	$15.640 \pm 2.82 \times 10^{-4}$	$18.814 \pm 3.34 \times 10^{-4}$	38.345	15.624	18.510
Fayetteville	FS11	325	158.8	17.2	11.5	14.0	6.08	$38.896 \pm 6.05 \times 10^{-4}$	$15.755 \pm 2.06 \times 10^{-4}$	$20.597 \pm 2.44 \times 10^{-4}$	38.332	15.647	18.480
Stanley	Stanley 1	330	83.6	13.0	7.3	1.6	0.69	$39.162 \pm 9.87 \times 10^{-4}$	$15.668 \pm 3.48 \times 10^{-4}$	$18.961 \pm 3.98 \times 10^{-4}$	38.692	15.651	18.639
Stanley	Stanley 2	330	52.3	5.9	4.9	1.5	0.23	$39.315 \pm 7.32 \times 10^{-4}$	$15.691 \pm 2.70 \times 10^{-4}$	$19.495 \pm 2.80 \times 10^{-4}$	38.630	15.657	18.830
Stanley	Stanley 3	330	62.9	13.5	7.5	1.4	0.67	$39.222 \pm 8.91 \times 10^{-4}$	$15.679 \pm 3.08 \times 10^{-4}$	$18.781 \pm 3.62 \times 10^{-4}$	38.758	15.666	18.526
Stanley	Stanley 4	330	101.2	18.3	20.0	3.4	0.29	$39.384 \pm 8.35 \times 10^{-4}$	$15.688 \pm 3.29 \times 10^{-4}$	$19.032 \pm 3.50 \times 10^{-4}$	38.469	15.664	18.556
Stanley	Stanley 4 (D)	330	73.8	10.9	8.3	1.8	n.d.	$39.348 \pm 7.22 \times 10^{-4}$	$15.696 \pm 2.81 \times 10^{-4}$	$18.993 \pm 3.23 \times 10^{-4}$	38.716	15.675	18.574
Chattanooga	CS1	360	151.6	17.9	9.7	40.4	7.60	$38.796 \pm 6.89 \times 10^{-4}$	$16.037 \pm 2.72 \times 10^{-4}$	$25.818 \pm 3.76 \times 10^{-4}$	38.306	15.715	19.534
Chattanooga	CS2	360	66.4	22.1	12.5	21.4	3.63	$38.895 \pm 6.75 \times 10^{-4}$	$15.797 \pm 2.55 \times 10^{-4}$	$21.477 \pm 3.48 \times 10^{-4}$	38.412	15.666	18.924
Chattanooga	CS3	360	85.2	8.3	10.4	15.9	3.44	$39.125 \pm 6.23 \times 10^{-4}$	$15.842 \pm 2.36 \times 10^{-4}$	$22.214 \pm 2.79 \times 10^{-4}$	38.041	15.580	17.103
Chattanooga	CS4	360	245.3	15.2	12.7	12.2	3.43	$39.182 \pm 8.23 \times 10^{-4}$	$15.785 \pm 2.86 \times 10^{-4}$	$21.174 \pm 3.89 \times 10^{-4}$	38.468	15.677	19.065
Chattanooga	CS5	360	76.6	20.0	12.9	11.7	3.66	$38.996 \pm 1.11 \times 10^{-3}$	$15.738 \pm 3.45 \times 10^{-4}$	$20.375 \pm 4.47 \times 10^{-4}$	38.453	15.660	18.853
Chattanooga	CS6	360	126.4	25.9	12.3	17.4	1.91	$38.848 \pm 6.40 \times 10^{-4}$	$15.729 \pm 2.57 \times 10^{-4}$	$20.087 \pm 3.67 \times 10^{-4}$	38.451	15.641	18.358
Chattanooga	CS7	360	112.8	15.8	10.7	31.0	4.80	$38.861 \pm 1.05 \times 10^{-3}$	$15.910 \pm 4.58 \times 10^{-4}$	$23.830 \pm 7.05 \times 10^{-4}$	38.261	15.636	18.473
Chattanooga	CS7 (R)	360	113.3	15.9	11.1	32.4	n.d.	n.d.	n.d.	n.d.	n.d.	n.d.	n.d.

Chattanooga	CS8	360	56.1	17.4	13.6	6.7	2.30	39.153 ± 7.61 × 10^{-4}	15.702 ± 2.51 × 10^{-4}	19.688 ± 2.92 × 10^{-4}	38.495	15.651	18.699
Chattanooga	CS9	360	57.6	29.3	13.6	7.0	2.50	38.847 ± 7.70 × 10^{-4}	15.681 ± 3.05 × 10^{-4}	19.226 ± 3.42 × 10^{-4}	38.461	15.650	18.619
Chattanooga	CS10B	360	45.0	62.1	14.9	15.3	2.92	40.806 ± 6.82 × 10^{-4}	15.897 ± 2.19 × 10^{-4}	21.876 ± 2.93 × 10^{-4}	40.594	15.863	21.208
Chattanooga	CS11	360	68.5	28.1	14.5	9.6	2.87	38.863 ± 7.05 × 10^{-4}	15.694 ± 2.36 × 10^{-4}	19.520 ± 3.13 × 10^{-4}	38.434	15.649	18.641
Chattanooga	CS12	360	77.0	24.0	14.9	10.5	2.47	38.900 ± 6.97 × 10^{-4}	15.700 ± 2.52 × 10^{-4}	19.638 ± 3.61 × 10^{-4}	38.379	15.642	18.515
Chattanooga	CS13	360	53.9	15.3	14.6	6.4	1.93	39.291 ± 7.85 × 10^{-4}	15.710 ± 2.53 × 10^{-4}	19.835 ± 3.06 × 10^{-4}	38.490	15.655	18.749
New Albany	Ceja Morris no. 1	360	86.7	23.1	5.6	12.6	5.72	38.642 ± 8.68 × 10^{-4}	15.771 ± 3.20 × 10^{-4}	20.918 ± 3.71 × 10^{-4}	38.436	15.699	19.499
New Albany	Ceja Morris no. 1	360	83.1	21.9	5.1	11.5	n.d.	n.d.	n.d.	n.d.	n.d.	n.d.	n.d.
Polk Creek	PC1	445	3.4	6.3	1.6	5.8	2.27	38.552 ± 1.03 × 10^{-3}	16.103 ± 3.65 × 10^{-4}	26.762 ± 6.22 × 10^{-4}	38.324	15.970	24.183
Polk Creek	PC1 (R)	445	5.9	6.4	1.6	5.9	n.d.	n.d.	n.d.	n.d.	n.d.	n.d.	n.d.
Polk Creek	Polk Creek 1	445	3.6	1.2	1.8	2.6	0.23	39.966 ± 7.09 × 10^{-2}	16.251 ± 6.00 × 10^{-2}	26.537 ± 6.60 × 10^{-2}	38.503	15.924	20.168
Polk Creek	Polk Creek 1 (D)	445	3.9	1.2	2.0	2.7	n.d.	39.445 ± 4.88 × 10^{-3}	16.105 ± 1.50 × 10^{-3}	26.420 ± 3.53 × 10^{-3}	37.855	15.773	19.950
Womble	Womble 1	460	40.6	14.1	11.3	2.3	0.71	38.628 ± 1.06 × 10^{-3}	15.562 ± 3.78 × 10^{-4}	18.663 ± 3.81 × 10^{-4}	37.972	15.541	18.249
Womble	Womble 2	460	2.9	2.2	1.0	1.6	1.04	38.843 ± 1.36 × 10^{-3}	15.796 ± 4.76 × 10^{-4}	21.271 ± 6.72 × 10^{-4}	38.434	15.699	19.375
Womble	Womble 3	460	2.8	2.2	1.1	1.6	0.49	38.851 ± 1.74 × 10^{-3}	15.794 ± 5.74 × 10^{-4}	21.257 ± 5.98 × 10^{-4}	38.409	15.697	19.372
Womble	Womble 3 (D)	460	76.9	16.1	7.3	3.0	n.d.	38.612 ± 9.54 × 10^{-3}	15.595 ± 3.35 × 10^{-4}	18.731 ± 3.77 × 10^{-4}	38.237	15.571	18.257
Mazarn	Mazarn 1	475	93.3	2.0	3.3	2.1	0.38	39.432 ± 2.21 × 10^{-3}	15.807 ± 7.09 × 10^{-4}	21.576 ± 7.31 × 10^{-4}	37.976	15.662	18.736
Mazarn	Mazarn 2	475	82.1	5.2	5.4	1.6	1.10	38.989 ± 1.19 × 10^{-3}	15.630 ± 4.14 × 10^{-4}	19.583 ± 4.54 × 10^{-4}	38.125	15.590	18.806
Mazarn	Mazarn 3	475	4.0	0.9	0.6	0.3	8.75	39.328 ± 1.51 × 10^{-3}	15.670 ± 5.03 × 10^{-4}	19.628 ± 5.47 × 10^{-4}	38.791	15.627	18.774
Mazarn	Mazarn 4	475	47.0	4.5	5.1	1.1	1.31	38.935 ± 1.13 × 10^{-3}	15.540 ± 4.00 × 10^{-4}	18.511 ± 4.11 × 10^{-4}	37.998	15.509	17.891
Collier	Collier CS1	485	85.4	12.7	5.4	5.3	2.46	38.436 ± 7.60 × 10^{-4}	15.730 ± 3.05 × 10^{-4}	19.993 ± 3.55 × 10^{-4}	38.081	15.675	18.925
Collier	Collier CS1 (R)	485	86.6	12.7	5.4	5.3	n.d.	n.d.	n.d.	n.d.	n.d.	n.d.	n.d.
Tunnel City	UPH-658	510	17.6	3.3	4.0	0.8	1.61	38.704 ± 9.25 × 10^{-4}	15.332 ± 3.33 × 10^{-4}	18.203 ± 3.76 × 10^{-4}	37.711	15.299	17.565
Eau Claire	Hwy A2 520	510	11.4	3.5	4.3	0.4	1.42	40.500 ± 9.46 × 10^{-4}	15.694 ± 3.30 × 10^{-4}	20.008 ± 4.41 × 10^{-4}	39.457	15.678	19.677
Eau Claire	UPH-853	510	15.5	14.2	2.9	0.5	0.73	40.430 ± 9.22 × 10^{-4}	15.884 ± 3.12 × 10^{-4}	20.871 ± 4.33 × 10^{-4}	40.258	15.880	20.781
Eau Claire	UPH-977	510	22.6	3.6	1.8	0.4	0.22	41.721 ± 9.77 × 10^{-4}	15.796 ± 3.09 × 10^{-4}	21.742 ± 4.32 × 10^{-4}	41.267	15.781	21.463
Mt. Simon	UPH-1363	515	40.4	6.0	3.6	1.0	0.16	41.327 ± 7.62 × 10^{-4}	15.869 ± 2.77 × 10^{-4}	21.588 ± 3.65 × 10^{-4}	40.793	15.844	21.117

Notes: The approximate age (Ma) of deposition of each shale unit is also given
Abbreviations: (D) = duplicate, n.d. = no data, (R) = replicate, TOC = total organic carbon

The Pb isotope ratios of each ore district define a relatively linear trend with partial overlap (Heyl et al., 1966; Doe and Delevaux, 1972; Deloule et al., 1986; Crocetti et al., 1988; Kesler et al., 1994a, b; Goldhaber et al., 1995; Leach et al., 2005, 2010a; Potra and Moyers, 2017; Potra et al., 2018; Fig. 4). The linear Pb isotope patterns suggest two possible scenarios. Conventionally, they have been interpreted to indicate mixing of Pb from two distinct end members (Doe and Delevaux, 1972; Goldhaber et al., 1995; Tosdal et al., 1999). One end member must be highly radiogenic, with Pb isotope ratios equal to or higher than the highest measured value of the ores. The other end member must be less radiogenic, with Pb isotope ratios equal to or lower than the lowest measured value. Lead isotope compositions of the ores will be intermediate between the two sources. Mixing of the fluids at or near the site of ore precipitation is required to maintain any Pb isotope distinction and is evidence for multiple fluid inputs (Tosdal et al., 1999). Conversely, if the fluids mixed at a significantly distant location away from the site of ore mineralization, they could adopt a homogeneous isotopic signature (Tosdal et al., 1999).

An alternative scenario is that the linear array represents a "pseudoisochron" (Jones et al., 2017). The slope of the linear trend defined by the Pb isotope ratios provides a model age of the radiogenic Pb. For Northern Arkansas ores, the slope is 0.0747 (Bottoms et al., 2019), which corresponds to an age of about 1.05 Ga. Southeast Missouri ores yield a slope of 0.073, which corresponds to a source age of 1.01 Ga (Crocetti et al., 1988). This may suggest input of Pb from an older source. The Precambrian crystalline basement that underlies the younger Phanerozoic sedimentary strata has been a hypothesized source in previous work (Crocetti et al., 1988; Goldhaber et al., 1995; Potra and Moyers, 2017; Field et al, 2018; Potra et al., 2018; Bottoms et al., 2019).

Studies in the Northern Arkansas and the Tri-State mining districts suggest that radiogenic shales, such as the Chattanooga Shale, may act as a less radiogenic end member source that mixed with a more radiogenic source to generate the observed Pb isotope ratios (Bottoms et al., 2019; Simbo et al., 2019). However, another possibility is that organic-rich shales are the only source of ore Pb. Shales consist of a wide array of organic molecules, each with their own thermal dissociation properties. Therefore, breaking down, or "cracking," these organic molecules may cover varying ranges of temperatures. Uranium, Th, and Pb associated with these molecules may thus yield Pb of different isotopic compositions at the time the organic molecules break down. This Pb may selectively and progressively be released into aqueous solution. Therefore, the Pb isotope compositions of the hydrothermal fluids interacting with organic-rich shales may evolve over time, closely approximating the isotopic composition of the released Pb at various times. The Pb isotope signatures of the hydrothermal fluids may therefore show apparent end members, without the need to have mixing of fluids from separate sources (Bottoms et al., 2019). Chick et al. (2021) analyzed the Pb isotope compositions of the Paleozoic carbonates, chert, and tuff of the southern Ozarks and Ouachita Mountain provinces, concluding that the rocks hosting the Northern Arkansas and the Tri-State ores contained relatively low Pb concentrations with highly radiogenic signatures. They concluded that the host rocks were not a viable source of the Pb ion, but these ions were likely deposited within the carbonate host rock via hydrothermal fluids.

On the uranogenic Pb isotope diagrams (^{207}Pb/^{204}Pb vs. ^{206}Pb/^{204}Pb), most of the shale samples from the Ouachita Mountains, the Ozark dome, and the Cherokee and Forest City basins analyzed in this study plot between the upper crust and orogenic growth curves of Zartman and Doe (1981) and to the left of the 0 Ma value of these curves (Fig. 4A, C). In contrast, the Ordovician Polk Creek Shale samples and one Devonian-Mississippian Chattanooga sample display highly radiogenic values and plot to the right of the 0 Ma value of the growth curves (Fig. 4A). Most of the Cambrian and Devonian-Mississippian samples from the Illinois basin display more radiogenic values and also plot to the right of the 0 Ma value of the growth curves (Fig. 4E). The orogenic growth curve approximates the average crustal growth curve of Stacey and Kramers (1975). For rocks or ores, deviations of Pb isotope values from those of the average crustal growth curves require geologic events that fractionated U-Th-Pb from those reservoirs with typical average crustal values (Tosdal et al., 1999). The average continental crust has a U/Pb value of 9.74 (Stacey and Kramers, 1975; Doe and Zartman, 1979). Lead isotope compositions lying at higher or lower ^{207}Pb/^{204}Pb at a given ^{206}Pb/^{204}Pb indicate that this Pb evolved in environments with U/Pb values higher or lower than that of the average crust (Tosdal et al., 1999).

On the thorogenic Pb isotope diagrams (^{208}Pb/^{204}Pb vs. ^{206}Pb/^{204}Pb), most of the shale samples from the Ouachita Mountains and the Ozark dome scatter above the orogenic growth curve, whereas some plot below the upper crust growth curve and plot to the left of the 0 Ma value of these curves (Fig. 4B). In contrast, the Ordovician Polk Creek Shale samples and one Devonian-Mississippian Chattanooga sample display highly radiogenic values and plot to the right of the 0 Ma value of the growth curves (Fig. 4B). The Cherokee and Forest City basin samples plot between the upper crust and orogenic growth curves and to the left of the 0 Ma value of these curves (Fig. 4D). Most of the Cambrian and Devonian-Mississippian samples from the Illinois basin display more radiogenic values and plot to the right of the 0 Ma value of the growth curves (Fig. 4E). Average continental crust has a Th/U value of 3.8 (Stacey and Kramers, 1975; Doe and Zartman, 1979). Lead isotope compositions lying at higher or lower ^{208}Pb/^{204}Pb at a given ^{206}Pb/^{204}Pb indicate that this Pb evolved in environments with Th/U values higher or lower than that of the average crust (Tosdal et al., 1999).

In general, most analyzed samples plot between the 8 and 0 Ga values of the growth curves (Fig. 4). However, a few samples exhibit whole-rock ratios that correlate with older Pb (~0.8 Ga and older), noticed in the Tunnel City Shale (Cambrian) and selected samples of the Chattanooga (Devonian) and Fayetteville shales (Mississippian). In contrast, most Illinois basin samples (New Albany, Eau Claire, and Mt. Simon shales) and the Polk Creek Shales (Ordovician) display future ages.

In comparison, the ores from the midcontinent mining districts are highly radiogenic and plot along a linear trend on both covariate Pb isotope diagrams (Fig. 4). Several samples of the Polk Creek, Chattanooga, Mt. Simon, and Eau Claire shales are the only ones whose Pb isotope signatures are closely akin to those of the ores (Fig. 4A, B, E, F). However, the resemblance is noticed either on the uranogenic diagram (Fig. 4A) or on the thorogenic diagram (Fig. 4F). The only exceptions are represented by one sample of the Chattanooga Shale (Fig. 4A, B) and one sample of the Eau Claire Formation (Fig. 4E, F).

The Cambrian Mt. Simon and Eau Claire shale samples, located proximal to the Upper Mississippi Valley mining district, have highly radiogenic Pb isotope signatures (Fig. 4E, F) but low Pb concentrations (<14 ppm). Similarly, samples of the Ordovician Polk Creek shales also display elevated uranogenic Pb isotope signatures (Fig. 4A, B) and low Pb concentrations (<16 ppm). The Devonian-Mississippian Chattanooga and New Albany shales yield higher Pb concentrations (ranging from 8 to 62 ppm and averaging 23 ppm). The only Chattanooga Shale with Pb concentrations greater than 29 ppm is a sample from the basal beds of the formation. This basal Chattanooga sample also has Pb ratios that are highly radiogenic (Fig. 4A, B), indicating direct interaction with hydrothermal fluids. It is therefore possible that these basal beds of the Chattanooga Shale might have contributed the ore Pb to the hydrothermal fluids that precipitated the MVT ores.

Although the Pb concentrations in the analyzed shales vary, with most shale samples containing up to 30 ppm Pb, the Pennsylvanian shales characterized by high total organic carbon content (>5 wt %) have up to 240 ppm of Pb. These Pb-rich shales indicate they generally formed under anoxic conditions, likely conducive to the preservation of organic carbon that ultimately bound with Pb ions at low temperatures (Tosdal et al., 1999). All Pennsylvanian shales in this study indicate they possessed average or near average crustal abundances of ^{235}U, ^{238}U, and ^{232}Th during their deposition (Fig. 4C, D). Unlike the shale samples from the Ouachita Mountains and the Ozark dome, these shales have very similar Pb isotope ratios and plot in a narrow field, suggesting a common Pb source. The Pb isotope ratios of a Chattanooga Shale sample resemble those of select Fayetteville Shale samples; they plot toward the 1.2 Ga value of the upper crust growth curve, corresponding to Precambrian-age Pb and suggesting a potentially deeper, igneous source(s) for the Pb in these rocks (Fig. 4A-D). However, it is unlikely that the Precambrian Pb was deposited contemporaneously with sedimentation, as both the Chattanooga and Fayetteville shales would have to share a Precambrian sediment source. Whereas the Fayetteville Shale had influence from a northerly sediment source, ancient Pb is not discernible in the Cambrian shales of the northern midcontinent, and the Pb isotope signatures do not exhibit similarity between these shales (Xie et al., 2016). Therefore, it is possible that some Precambrian Pb was concentrated in the shales during the migration of Pb-bearing fluids, potentially resulting from fluid mixing or the migration of ancient Pb from a local source(s). Moreover, the slope of the linear trend defined by the Pb isotope ratios of the southern Ozark region ores (Northern Arkansas and Tri-State districts) corresponds to an age of about 1.2 Ga, suggesting input of Pb from a Precambrian source (Chick et al., 2021). In this case, the observed linear array suggests a possible inheritance from the local basement (Chick et al., 2021).

Whereas the ores preferentially form within zones characterized by high permeability and porosity (e.g., vugs, breccias, etc.), shales may contain limited quantities of ore mineralization but often function as aquitards owing to their low permeability, limiting the migration of hydrothermal fluids. Consequently, the role of shales as a sink for metals would be most evident along the upper or basal beds of the shale, which have the most interaction with hydrothermal fluids. Certain shales may acquire elevated Pb isotope signatures and elevated Zn concentrations along these portions of the shale, rather than in the middle portions. As mentioned above, most of the analyzed shales do not reflect the elevated abundances of radiogenic Pb characteristic of the regional ores, further suggesting their role is more likely as a sink rather than a source of Pb. However, extensions of the lines of best fit through the Pb isotope ratios of the ores suggest that some shales may serve as the lesser radiogenic Pb source(s) that mixed with a highly radiogenic Pb whose source still lays further afield. It appears that Pb in the Chattanooga Shale is a good candidate for the Tri-State district ore Pb (Fig. 4A-D). This is apparent in the thorogenic and uranogenic diagrams. It is important to note that the limited number of analyzed samples for some shale formations restricts making comprehensive inferences, but the samples are valuable for comparative purposes. Additional sampling may also help refine the spatial resolution across the study area and vertically within individual stratigraphic sequences.

Conclusions

The highly radiogenic characteristics of MVT ores in the midcontinent districts are indicative of a Pb source(s) enriched in ^{238}U, ^{235}U, and ^{232}Th relative to the upper crust and orogenic growth curves. The Pb isotope ratios of most ores suggest the potential involvement of a single highly radiogenic source mobilized by hydrothermal fluids, or the mixing of at least two sources of Pb with differing radiogenic signatures. The analysis of shale samples revealed variations in Pb concentrations and isotopic compositions across different Cambrian- to Pennsylvanian-age shales. Shales with high organic carbon content, particularly those of Pennsylvanian age, displayed elevated Pb abundances, suggesting their formation under anoxic conditions conducive to the preservation of organic carbon binding with Pb ions. However, the Pb isotopes in the black shales are generally less radiogenic than the ores, which suggests that they were not a source of radiogenic Pb. This is because they have Pb ratios corresponding to their age of depositions, suggesting they were deposited in the sediment when the shales formed and may have been the product of the radioactive decay of dissolved U and Th that adsorbed in the sediment during deposition of the shales.

There are some samples of the Chattanooga Shale and Polk Creek Shale that have significant quantities of radiogenic Pb that more closely resemble those of the MVT ores. It would be expected that the shales would plot similarly with the ores if the shales were the single source of radiogenic Pb. However, they generally do not fit well with the isotopic trends of the ores. This suggests that certain shales, such as the Chattanooga Shale and the Polk Creek Shale, may have directly interacted with the hydrothermal fluids that precipitated the MVT ores. Some shales may have acted as an aquitard as the hydrothermal fluids were migrating through the subsurface, leading some shales to become more enriched in radiogenic Pb than others.

Other potential sources for the radiogenic Pb may be deep basinal migration of brines transporting Pb from the basement via faults associated with the Ouachita orogeny. Pb isotope analyses of basement rock from the midcontinent could also provide additional information regarding the source of the radiogenic Pb if fluids migrated through basement faults during the Ouachita orogeny. Further sampling for Pb from additional shale units, as well as from individual stratigraphic intervals of shales and other stratigraphic units, may provide further understanding of the migration of Pb-bearing hydrothermal fluids associated with the Ouachita orogeny and MVT ore mineralization.

Acknowledgments

The study was funded by National Science Foundation (NSF) grant 1952088. Core samples were provided by the Wisconsin Geological and Natural History Survey. Thanks to Erik Pollock and Barry Shaulis for their lab assistance in analyses using the ThermoScientific iCAP Q ICP-MS and Nu Plasma MC-ICP-MS instruments. Thanks are also extended to Will Hadley, Jackson Copeland, and Alex Goodsuhm for field and lab support, as well as to Bryan Bottoms and Christophe Simbo for sample collection.

REFERENCES

Anderson, K.H., and Wells, J.S., 1968, Forest City basin of Missouri, Kansas, Nebraska, and Iowa: American Association of Petroleum Geologists Bulletin, v. 52, no. 2, p. 264–281.

Appold, M.S., and Garven, G., 1999, The hydrology of ore formation in the southeast Missouri district: Numerical models of topography-driven fluid flow during the Ouachita orogeny: Economic Geology, v. 94, p. 913–936.

Appold, M.S., and Nunn, J.A., 2005, Hydrology of the western Arkoma basin and Ozark platform during the Ouachita orogeny: Implications for Mississippi Valley-type ore formation in the Tri-State Zn-Pb district: Geofluids, v. 5, p. 308–325.

Arbenz, J.K., 1989, The Ouachita system, *in* Bally, A.W., and Palmer, A.R., eds., The geology of North America—an overview: Boulder, Colorado, Geological Society of America, p. 371–396.

Arne, D.C., 1992, Evidence from apatite fission-track analysis for regional Cretaceous cooling in the Ouachita Mountain fold belt and Arkoma basin of Arkansas: American Association of Petroleum Geologists Bulletin, v.76, no. 3, p. 392–402.

Arne, D.C., Green, P.F., and Duddy, I.R., 1990, Thermochronologic constraints on the timing of Mississippi Valley-type ore formation from apatite fission track analysis: International Journal of Radiation Applications and Instrumentation Part D. Nuclear Tracks and Radiation Measurements, v. 17, no. 3, p. 319–323.

Arsdale, R., and Cupples, W., 2013, Late Pliocene and Quaternary deformation of the Reelfoot rift: Geosphere, v. 9, no. 6, p. 1819–1831.

Basuki, N.I., and Spooner, E.T.C., 2004, A review of fluid inclusion temperatures and salinities in Mississippi Valley-type Zn-Pb deposits: Identifying thresholds for metal transport: Exploration and Mining Geology, v. 11, p. 1–17.

Bottoms, B., Potra, A., Samuelsen, J.R., and Schutter, S.R., 2019, Geochemical investigations of the Woodford-Chattanooga and Fayetteville Shales: Implications for genesis of the Mississippi Valley-type zinc-lead ores in the southern Ozark region and hydrocarbon exploration: American Association of Petroleum Geologists Bulletin, v. 103, no. 7, p. 1745–1768.

Bourcier, W.L., and Barnes, H.L., 1987, Ore solution chemistry; VII, Stabilities of chloride and bisulfide complexes of zinc to 350°C: Economic Geology, v. 82, no. 7, 1839–1863.

Bradley, D.C., and Leach, D.L., 2003, Tectonic controls of Mississippi Valley-type lead-zinc mineralization in orogenic forelands: Mineralium Deposita, v. 38, no. 6, p. 652–667.

Brannon, J.C., Podosek, F.A., and Cole, S.C., 1996, Radiometric dating of Mississippi Valley-type ore deposits: Carbonate-hosted lead-zinc deposits: Society of Economic Geologists Guidebook Series, v. 22, p. 536–545.

Cannon, R.S., and Pierce, A.P., 1969, Lead isotope guides for Mississippi Valley lead-zinc exploration: A review of correlations of isotopic compositions of ore-lead and tonnages of known ore in Mississippi Valley lead-zinc deposits: U.S. Geological Survey, Bulletin 1312-G, p. 1–20.

Carne, R.C., and Cathro, R.J., 1982, Sedimentary exhalative (SEDEX) zinc-lead-silver deposits, northern Canadian Cordillera: Canadian Institute of Mining, Metallurgy and Petroleum Bulletin, v. 840, p. 102–116.

Chick, J., McKim, S.E., Potra, A., Manger, W.L., and Samuelsen, J.R., 2021, Radiogenic Pb enrichment of Mississippi Valley-type metallic ore deposits, southern Ozarks: Constraints based on geochemical studies of source rocks and their diagenetic history: Geosciences, v. 11, no. 4, article 172, p. 1–22.

Chinn, A.A.V., and König, R.H., 1973, Stress inferred from calcite twin lamellae in relation to regional structure of northwest Arkansas: Geological Society of America Bulletin, v. 84, no. 11, p. 3731–3736.

Coveney, R.M., Jr., 2003, Metalliferous Paleozoic black shales and associated strata: Geological Association of Canada, GeoText 4, p. 135–144.

Coveney, R.M., Jr., and Glascock, M.D., 1989, A review of the origins of metal-rich Pennsylvanian black shales central U.S.A., with an inferred role for basinal brines: Applied Geochemistry, v. 4, p. 347–367.

Coveney, R.M., Jr., Watney, W.L., and Maples, C.G., 1989, Rates and durations for accumulation of Pennsylvanian black shales in the midwestern United States: Kansas Geological Survey Subsurface Geology, v. 12, p. 73–76.

Crocetti, C.A., Holland, H.D., and McKenna, L.W., 1988, Isotopic comparison of lead in galenas from the Viburnum trend, Missouri: Economic Geology, v. 83, no. 2, p. 355–376.

Deloule, E., Allegre, C.J., and Doe, B.R., 1986, Lead and sulfur isotope microstratigraphy in galena crystals from Mississippi Valley-type deposits: Economic Geology, v. 81, no. 6, p. 1307–1321.

Devera, J.A., and Fraunfelter, G.H., 1988, Middle Devonian paleogeography and tectonic relationships east of the Ozark dome, southeastern Missouri, southwestern Illinois and parts of southwestern Indiana and western Kentucky: Canadian Society of Petroleum Geologists Memoirs, v. 14, no. 2, p. 179–196.

Dickin, A.P., 2005, Radiogenic isotope geology: Cambridge, Cambridge University Press, 482 p.

Doe, B.R., and Delevaux, M.H., 1972, Source of lead in southeast Missouri galena ores: Economic Geology, v. 67, no. 4, p. 409–425.

Doe, B.R., and Zartman, R.E., 1979, Plumbotectonics I, The Phanerozoic, *in* Barnes, H.L., ed., Geochemistry of hydrothermal ore deposits: New York, Wiley-Interscience, p. 22–70.

Doe, B.R., Stuckless, J.S., and Delevaux, M.H., 1983, The possible bearing of the granite of the UPH deep drill holes, northern Illinois, on the origin of Mississippi Valley ore deposits: Journal of Geophysical Research, v. 88, no. B9, p. 7335-7345.

Ervin, C.P., and McGinnis, L.D., 1975, Reelfoot rift: Reactivated precursor to the Mississippi embayment: Geological Society of America Bulletin, v. 86, no. 9, p. 1287–1295.

Field, J.D., Appold, M.S., Renson, V., and Coveney, R.M., Jr., 2018, Lead and sulfur isotope composition of trace occurrences of Mississippi Valley-type mineralization in the U.S. midcontinent: Journal of Geochemical Exploration, v. 184, p. 66–81.

Field, J.D., Appold, M.S., Coveney, R.M., Jr., and Bodnar, R.J., 2020, Geochemical characteristics of trace occurrences of Mississippi Valley-type mineralization in the U.S. mid-continent: Implications for deposit growth: Journal of Geochemical Exploration, v. 213, no. 106514, p. 1–23.

Garven, G., Ge, S., Person, M.A., and Sverjensky, D.A., 1993, Genesis of stratabound ore deposits in the Midcontinent basins of North America. 1. The role of regional groundwater flow: American Journal of Science, v. 293, no. 6, p. 497–568.

Goldhaber, M.B., Church, S.E., Doe, B.R., Aleinikoff, J.N., Brannon, J.C., Podosek, F.A., Mosier, E.L., Taylor, C.D., and Gent, C.A., 1995, Lead and sulfur isotope investigation of Paleozoic sedimentary rocks from the southern Midcontinent of the United States; implications for paleohydrology and ore genesis of the Southeast Missouri lead belts: Economic Geology, v. 90, no. 7, p. 1875–1910.

Harris, J.W., 1985, Stratigraphy of the Cherokee Group, southeastern Kansas, *in* Watney, W.L., Walton, A.W., and Doveton, J., eds., Core studies in Kansas. Sedimentology and diagenesis of economically important rock strata in Kansas: Kansas Geological Survey Subsurface Geology, v. 6, p. 66–73.

Hatcher, R.D., Jr., 2002, Alleghanian (Appalachian) orogeny, a product of zipper tectonics: rotational transpressive continent-continent collision and closing of ancient oceans along irregular margins, *in* Martínez Catalán, J.R., Hatcher, R.D.J., Arenas, R., and Díaz García, F., eds., Variscan-Appalachian dynamics: The building of the late Paleozoic basement: Boulder, Colorado, Geological Society of America, p. 199–208.

Hay, R.L., Liu, J., Barnstable, D.C., Deino, A., Kyser, T.K., Childers, G.A., and Walker, W.T., 1995, Dates and mineralogic results from claypods of Mine 29 and Sweetwater mine, Viburnum trend, Missouri, *in* Leach, D.L., and Goldhaber, M.B., eds., Extended abstracts: International field conference on carbonate-hosted lead-zinc deposits: St. Louis, Missouri, Society of Economic Geologists, p. 124–126.

Henley, R.W., Truesdell, A.H., Barton, P.B., and Whitney, J.A., eds., 1984, Fluid-mineral equilibria in hydrothermal systems: Reviews in Economic Geology, v. 1, 13 p.

Heyl., A.V., Delevaux, M.H., Zartman, R.E., and Brock, M.R., 1966, Isotopic study of galenas from the upper Mississippi Valley, the Illinois-Kentucky, and some Appalachian Valley mineral districts: Economic Geology, v. 61, no. 5, p. 933–961.

Houseknecht, D.W., and Matthews, S.M., 1985, Thermal maturity of Carboniferous strata, Ouachita Mountains: American Association of Petroleum Geologists Bulletin, v. 69, no. 3, p. 335–345.

Houtermans, F.G., 1953, Determination of the age of the earth from the isotopic composition of meteoric lead: Il Nuovo Cimento, v. 10, no. 1, p. 1623–1633.

Hudson, M.R., 2000, Coordinated strike-slip and normal faulting in the southern Ozark dome of northern Arkansas: Deformation in a late Paleozoic foreland: Geology, v. 28, no. 6, p. 511–514.

Jewett, J.M., 1933, Some details of the stratigraphy of the Bronson Group of the Kansas Pennsylvanian: Transactions of the Kansas Academy of Science, v. 36, p. 131–136.

Jones, D.S., Turner, B.L., Buikstra, J.E., and Kamenov, G.D., 2017, Investigating the identities of isolated crania in the Lower Illinois River Valley through multi-isotopic analysis: Journal of Archaeological Science, v. 13, p. 312–321.

Jopling, D.W., and Cashion, K., 1959, Regional gravity of Kansas: State Geological Survey of Kansas Bulletin, v. 137, p. 121–133.

Kesler, S.E., Appold, M.S., Cumming, G.L., and Krstic, D., 1994a, Lead isotope geochemistry of Mississippi Valley-type mineralization in the central Appalachians: Economic Geology, v. 89, no. 7, p. 1492–1500.

Kesler, S.E., Cumming, G.L., Krstic, D., and Appold, M.S., 1994b, Lead isotope geochemistry of Mississippi Valley-type deposits of the southern Appalachians: Economic Geology, v. 89, no. 2, p. 307–321.

Klein, G.deV., and Hsui, A.T., 1987, Origin of cratonic basins: Geology, v. 15, p. 1094–1098.

Kochenov, A.V., and Baturin, G.N., 2002, The paragenesis of organic matter, phosphorus, and uranium in marine sediments: Lithology and Mineralogy Research, v. 37, no. 2, p. 107–120, English translation.

Kolata, D.R., and Nelson, W.J., 1990a, Tectonic history of the Illinois basin, *in* Leighton, M.W., Kolata, D.R., Oltz, D.F., and Eidel, J.J., eds., Interior cratonic basins: American Association of Petroleum Geologists Memoirs, v. 51, p. 263–286.

——1990b, Basin-forming mechanisms of the Illinois basin, *in* Leighton, M.W., Kolata, D.R., Oltz, D.F., and Eidel, J.J., eds., Interior cratonic basins: American Association of Petroleum Geologists Memoirs, v. 51, p. 287–298.

Lange, S., Chaudhuri, S., and Clauer, N., 1983, Strontium isotopic evidence for the origin of barites and sulfides from the Mississippi Valley-type ore deposits in southeast Missouri: Economic Geology, v. 78, no. 6, p. 1255–1261.

Leach, D.L., and Sangster, D.F., 1993, Mississippi Valley-type lead-zinc deposits: Mineral deposit modeling: Geological Association of Canada, Special Paper 40, p. 289–314.

Leach, D.L., Nelson, R.C., and Williams, D., 1975, Fluid inclusion studies in the northern Arkansas zinc district: Economic Geology, v. 70, p. 1084–1091.

Leach, D.L., Bradley, D., Lewchuk, M.T., Symons, D.T.A., de Marsily, G., and Brannon, J., 2001, Mississippi Valley-type lead-zinc deposits through geological time: Implications from recent age-dating research: Mineralium Deposita, v. 36, no. 8, p. 711–740.

Leach, D.L., Sangster, D.F., Kelley, K.D., Large, R.R., Garven, G., Allen, C.R., Gutzmer, J., and Walters, S., 2005, Sediment-hosted lead-zinc deposits: A global perspective: Economic G 100th Anniversary Volume, p. 561–607.

Leach, D.L., Taylor, R.D., Fey, D.L., Diehl, S.F., and Saltus, R.W., 2010a, A deposit model for Mississippi Valley-type lead-zinc ores: U.S. Geological Survey, Scientific Investigations Report, v. 2010-5070-A, p. 1–52.

Leach, D.L., Bradley, D.C., Huston, D., Pisarevsky, S.A., Taylor, R.D., and Gardoll, S.J., 2010b, Sediment-hosted lead-zinc deposits in Earth history: Economic Geology, v. 105, p. 593–625.

Leighton, M.W., and Kolata, D.R., 1990, Selected interior cratonic basins and their place in the scheme of global tectonics: A synthesis: American Association of Petroleum Geologists Memoirs, v. 51, p. 729–797.

Lowell, G.R., and Young, G.J., 1999, Interaction between coeval mafic and felsic melts in the St. Francois terrane of Missouri, USA: Precambrian Research, v. 95, no. 1–2, p. 69–88.

McBride, J.H., and Nelson, W.J., 1999, Style and origin of mid-Carboniferous deformation in the Illinois basin, USA—ancestral Rockies deformation?: Tectonophysics, v. 305, no. 1–3, p. 249–273.

McFarland, J.D., 2004, Stratigraphic summary of Arkansas: Arkansas Geological Survey Information Circular, v. 36, 38 p.

Meert, J.G., and Stuckey, W., 2002, Revisiting the paleomagnetism of the 1.476 Ga St. Francois Mountains igneous province, Missouri: Tectonics, v. 21, no. 2, p. 1–19.

Montanez, I.P., 1994, Late diagenetic dolomitization of Lower Ordovician, Upper Knox carbonates: A record of the hydrodynamic evolution of the southern Appalachian basin: American Association of Petroleum Geologists Bulletin, v. 78, no. 8, p. 1210–1239.

Moore, R.C., 1932, Kansas, Missouri, Nebraska: Kansas Geological Society, 6th Annual Field Conference, 1932, Guidebook, 125 p.

Morris, R.C., 1971, Stratigraphy and sedimentology of Jackfork Group, Arkansas: American Association of Petroleum Geologists Bulletin, v. 55, no. 3, p. 387–402.

Nance, R.D., Gutiérrez-Alonso, G., Keppie, J.D., Linnemann, U., Murphy, J.B., Quesada, C., Strachan, R.A., and Woodcock, N.H., 2010, Evolution of the Rheic Ocean: Gondwana Research, v. 7, no. 2–3, p. 194–222.

Neir, A.O., 1938, Variations in the relative abundances of the isotopes of common lead from various sources: Journal of the American Chemical Society, v. 60, p. 1571–1576.

Nelson, K.D., and Zhang, J., 1991, A COCORP deep reflection profile across the buried Reelfoot rift, south-central United States: Tectonophysics v. 197, no. 2–4, p. 271-293.

Newell, K.D., 1995, Overview of petroleum geology and production in Kansas: Kansas Geological Survey Bulletin, v. 237, p. 2–6.

Owen, M.R., and Carozzi, A.V., 1986, Southern provenance of upper Jackfork Sandstone, southern Ouachita Mountains: Cathodoluminescence petrology: Geological Society of America Bulletin, v. 97, no. 1, p. 110–115.

Pan, H., Symons, D.T.A., and Sangster, D.F., 1990, Paleomagnetism of the Mississippi Valley-type ores and host rocks in the northern Arkansas and Tri-State districts: Canadian Journal of Earth Science, v. 27, p. 923–931.

Pan, H., Symons, D.T.A., and Sangster, D.F., 2011, Paleomagnetism of the Mississippi Valley-type ores and host rocks in the northern Arkansas and Tri-State districts: Canadian Journal of Earth Science, v. 27, no. 7, p. 923–931.

Parrish, S., and Arsdale, R., 2004, Faulting along the southeastern margin of the Reelfoot rift in northwestern Tennessee revealed in deep seismic-reflection profiles: Seismological Research Letters, v. 75, no. 6, p. 784–793.

Pin, C., Gannoun, A., and Dupont, A., 2014, Rapid, simultaneous separation of Sr, Pb, and Nd by extraction chromatography prior to isotope ratios determination by TIMS and MC-ICP-MS: Journal of Analytical Atomic Spectrometry, v. 29, no. 10, p. 1858–1870.

Plumlee, G.S., Leach, D.L., Hofstra, A.H., Landis, G.P., Rowan, E.L., and Viets, J.G., 1994, Chemical reaction path modeling of ore deposition in Mississippi Valley-type Pb-Zn deposits of the Ozark region, U.S. Midcontinent: Economic Geology, v. 89, no. 6, p. 1361–1383.

Potra, A., and Moyers, A., 2017, Constraints on the sources of ore metals in Mississippi Valley-type deposits in central and east Tennessee, USA, using Pb isotopes: Ore Geology Reviews, v. 81, p. 201–210.

Potra, A., Garmon, W.T., Samuelsen, J.R., Wulff, A., and Pollock, E.D., 2018, Lead isotope trends and metal sources in the Mississippi Valley-type districts from the mid-continent United States: Journal of Geochemical Exploration, v. 192, p. 174–186.

Powell, R., Will, T.M., and Phillips, G.N., 1991, Metamorphism in Archean greenstone belts: Calculated fluid compositions and implications for gold mineralization: Journal of Metamorphic Geology, v. 9, no. 2, p. 141–150.

Sargent, M.L., 1990, Sauk sequence: Cambrian system through Lower Ordovician series: American Association of Petroleum Geologists Memoirs, v. 51, p. 75–85.

Saxby, J.D., 1976, The significance of organic matter in ore genesis, *in* Wolf, K.H., ed., Handbook of strata-bound and stratiform ore deposits, v. 1, no. 2: Amsterdam, Elsevier, p. 111–133.

Schutter, S.R., 2015, Lead-zinc mineralization as an indicator of unconventional resources: Houston Geological Society Bulletin, v. 57, no. 9, p. 33–49.

Searight, W.V., 1955, Guidebook, field trip: Association of Missouri Geologists, Annual Meeting, 2nd, Geological Survey and Water Resources Report of Investigations, no. 20, 44 p.

Simbo, C.W., Potra, A., and Samuelsen, J.R., 2019, A geochemical evaluation of the genetic relationship between Ouachita Mountains Paleozoic rocks and the Mississippi Valley-type mineralization in the southern Ozark region, USA: Ore Geology Reviews, v. 112, article 103029, 18 p., doi: 10.1016/j.oregeorev.2019.103029.

Simonds, F.W., 1891, The geology of Washington County: Annual Report of the Geological Survey of Arkansas for 1888, v. 4, p. 1–154.

Stacey, J.S., and Kramers, J.D., 1975, Approximation of terrestrial lead isotope evolution by a two-stage model: Earth and Planetary Science Letters, v. 26, p. 207–221.

Stein, H.J., and Kish, S.A., 1985, The timing of ore formation in Southeast Missouri; Rb-Sr glauconite dating at the Magmont mine, Viburnum trend: Economic Geology, v. 80, no. 3, p. 739–753.

Sutherland, P.K., 1988, Late Mississippian and Pennsylvanian depositional history in the Arkoma basin area, Oklahoma and Arkansas: Geological Society of America Bulletin, v. 100, p. 1787–1802.

Symons, D.T.A., and Sangster, D.F., 1991, Paleomagnetic age of the central Missouri barite deposits and its genetic implications: Economic Geology, v. 86, no. 1, p. 1–12.

Symons, D.T.A., Lewchuk, M.T., and Leach, D.L., 1998, Age and duration of the Mississippi Valley-type mineralizing fluid flow event in the Viburnum trend, southeast Missouri, USA, determined from palaeomagnetism: Geological Society, London, Special Publications, v. 144, no. 1, p. 27–39.

Todt, W., Cliff, R.A., Hanser, A., and Hofmann, A.W., 1996, Evaluation of a ^{202}Pb-^{205}Pb double spike for high precision lead isotope analysis: American Geophysical Union Geophysical Monographs, v. 95, p. 429–437.

Tosdal, R.M., Wooden, J.L., and Bouse, R.M., 1999, Pb isotopes ore deposits and metallogenic terranes: Reviews in Economic Geology, v. 12, p. 1–28.

Wisniowiecki, M.J., van der Voo, R., McCabe, C., and Kelly, W.C., 1983, A Pennsylvanian paleomagnetic pole from the mineralized late Cambrian Bonneterre Formation, southeast Missouri: Journal of Geophysical Research, Solid Earth, v. 88, no. B8, p. 6540–6548.

Wood, S.A., Crerar, D.A., and Borcsik, M.P., 1987, Solubility of the assemblage pyrite-pyrrhotite-magnetite sphalerite-galena-gold-stibnite-bismuthinite-argentite-molybdenite in H_2O-NaCl-CO_2 solutions from 200 degrees to 350 degrees C: Economic Geology, v. 82, no. 7, p. 1864–1887.

Xie, X., Cains, W., and Manger, W.L., 2016, U-Pb detrital zircon evidence of transcontinental sediment dispersal: provenance of Late Mississippian Wedington Sandstone member, NW Arkansas: International Geology Review, v. 58, no. 15, p. 1951–1966.

Yardley, B.W.D., 2005, 100th anniversary special paper: Metal concentrations in crustal fluids and their relationship to ore formation: Economic Geology, v. 100, no. 4, p. 613–632.

York, D.A., Masliwec, A., Hall, C.M., Kuybida, P., Kenyon, W.J., Spooner, E.T.C., and Scott, S.D., 1981, The direct dating of ore minerals: Ontario Geological Survey, Miscellaneous Paper 98, p. 334–340.

Zartman, R.E., and Doe, B.R., 1981, Plumbotectonics—the model: Tectonophysics, v. 75, no. 1, p. 135–162.

Noah Morris received a B.S. degree in geology from the University of Oklahoma in 2010 and M.S. and Ph.D. degrees in geology from the University of Arkansas in 2017 and 2023, respectively. As a student he worked on the geochemistry of organic-rich shales. He has previously worked in the oil and gas industry for Geosearch Logging, ALS Empirica, and Impac Exploration.